
SSUL: Semantic Segmentation with Unknown Label for Exemplar-based Class-Incremental Learning

Sungmin Cha^{1,2,*}, Beomyoung Kim^{3,*}, YoungJoon Yoo^{2,3}, and Taesup Moon¹

¹ Department of Electrical and Computer Engineering, Seoul National University

² NAVER AI Lab, ³ Face, NAVER Clova

sungmin.cha@snu.ac.kr, {beomyoung.kim, youngjoon.yoo}@navercorp.com,
tmoon@snu.ac.kr

Abstract

This paper introduces a solid state-of-the-art baseline for a class-incremental semantic segmentation (CISS) problem. While the recent CISS algorithms utilize variants of the knowledge distillation (KD) technique to tackle the problem, they failed to fully address the critical challenges in CISS causing the catastrophic forgetting; the semantic drift of the background class and the multi-label prediction issue. To better address these challenges, we propose a new method, dubbed SSUL-M (Semantic Segmentation with Unknown Label with Memory), by carefully combining techniques tailored for semantic segmentation. Specifically, we claim three main contributions. (1) defining *unknown* classes within the background class to help to learn future classes (help plasticity), (2) *freezing* backbone network and past classifiers with binary cross-entropy loss and pseudo-labeling to overcome catastrophic forgetting (help stability), and (3) utilizing *tiny exemplar memory* for the first time in CISS to improve both plasticity and stability. The extensively conducted experiments show the effectiveness of our method, achieving significantly better performance than the recent state-of-the-art baselines on the standard benchmark datasets. Furthermore, we justify our contributions with thorough ablation analyses and discuss different natures of the CISS problem compared to the traditional class-incremental learning targeting classification. The official code is available at <https://github.com/clovaai/SSUL>.

1 Introduction

Class incremental learning (CIL) problem, in which a learner should incrementally learn newly arriving class objects while not “catastrophically” forgetting the past learned classes, is one of the fundamental, yet still open, problems in machine learning. After the seminal work, [27], most of the recent neural network-based CIL research has focused on the classification setting, and various approaches have been proposed to address the main challenge of the problem, the so-called plasticity-stability dilemma, *e.g.*, [20, 30, 12, 1, 2, 8], to name a few.

The CIL framework has been extended to more complex semantic segmentation tasks [24, 3, 7], motivated by the practical need in various applications such as autonomous driving. One of the key additional difficulties of the class-incremental semantic segmentation (CISS) problem lies in the semantic drift of the background class present in the incrementally arriving training data. Namely, the label ‘background (BG)’ is assigned to all the pixels not included in the *current* class object region. The “BG” pixels belong to *three* categories: future object classes that the model does not yet observes, past object classes that are already learned, and the true background.

*Equal contribution.

A few recent works attempted to address the above semantic drift issue by leveraging and modifying the knowledge-distillation (KD) [20] technique, popular for CIL in standard image classification. Namely, the initiative study [24] modified the KD for CISS straightforwardly, and [3] proposed a strategy to incorporate the BG class probability in computing the cross-entropy and distillation losses. Furthermore, [7], the current state-of-the-art, utilized the pseudo-labeling of the BG pixels of the current task data with the model of the previous task using the cross-entropy loss, and it applies the multi-scale feature distillation scheme adopted from [8]. However, we argue that above works only partially addressed the BG label issue. That is, [3] naively *added* the class probabilities to modify the cross-entropy and distillation losses making it hard to have fine-grained learning of prediction probability for each class, each pixel. Moreover, [7] could only handle the BG class pixels to the *past* classes via pseudo-labeling and lacked any mechanism for handling the *future* class case, one possible option for the the BG class. Consequently, their CIL segmentation performance, measured by mean Intersection-over-Union (mIoU), has been significantly lower than the upper-bound, the case of joint-training with all the labels.

This paper first identifies that the multi-label prediction of semantic segmentation is another critical challenge of CISS and proposes SSUL-M (Semantic Segmentation with Unknown Label with Memory) to address the challenge. Specifically, Our contributions are summarized as follows. First, we introduce an additional “*Unknown*” class label assigned to the objects in the background, detected by the off-the-shelf saliency-map detector. We let the base feature extractor distinguish the representations of the potential future class objects and the actual background region by augmenting the BG label with this additional class. Second, we adopt the pseudo-labeling strategy as in [7] and further augment the BG & Unknown class labels with the past class labels, but with two essential differences in concrete learning strategies to stabilize the classification scores and improve the *precision* of the prediction. One is using the separate *sigmoid*, instead of the softmax, output classifier for each class so that the model can learn the logit score in an absolute sense per class. The other is *freezing* the base feature extractor and the classifiers for past classes after initial learning to strictly maintain the past classes’ knowledge. Third, we utilize an *exemplar memory* to store a tiny portion of training data, including past classes, as anchors and further improve the mIoU. Note that using the exemplar memory is a standard practice for CIL in classification but has been overlooked in CISS. Moreover, we show that the memory helps improve the mIoU for the *current* classes, in contrast to a common belief that it is a tool to prevent forgetting of past classes.

By integrating the above contributions, SSUL-M achieved the state-of-the-art performance on popular benchmarks with a *significantly large* margin over the recent baselines [3, 7], particularly when the number of incremental tasks gets larger. Furthermore, we conduct extensive ablation studies and both quantitative and qualitative analyses to convincingly highlight the strength of our method.

2 Related Work

Class Incremental Learning (CIL) CIL [28, 25] considers the setting in which new class objects arrive incrementally and the model needs to classify *all* the classes without storing all the past class data. It is well known that neural network-based CIL suffers from catastrophic forgetting [23], caused by the score bias toward the new classes due to the training data imbalance. Most CIL studies have focused on the classification tasks, and the exemplar-memory based methods combined with KD [30, 12, 1, 2, 8] achieved the state-of-the-art performance by re-balancing the biased predictions of the classifier.

Class Incremental Semantic Segmentation (CISS) Contrary to the current trend of CIL for classification, CIL for semantic segmentation have only focused on the setting without utilizing the exemplar-memory [24, 3, 7]. [3] first addressed the semantic drift of BG label, and [7] proposed to use pseudo-labels to augment the BG label, all without exemplar-memory. To our knowledge, we firstly use exemplar-memory and potential future classes in BG label to solve CISS.

Saliency Map Detection Salient object detection is a fundamental computer vision task that identifies the most visually distinctive objects in an image. We use the off-the-shelf saliency-map detector to define the *Unknown* class in the BG label. The early salient object detection method, DRFI [13], conducts a multi-level segmentation with a random forest regressor to detect a salient object. Recent deep neural network based method exploits rich multi-scale feature maps with short

connections [11] and pooling-based modules [21]. The saliency information has widely been utilized on various tasks. For example, the weakly-supervised semantic segmentation approaches [29, 31, 14] generate pseudo-labels filtering out the background regions using saliency map, and recent data augmentations [17, 16] also exploit the saliency information to find the optimal mixing of mask.

3 Proposed Method

3.1 Notations and Problem Setting

We consider exactly the same setting as considered in [3, 7]. In CISS, the learning happens with $t = 1, \dots, T$ incremental tasks. For each incremental state t , we observe a training dataset \mathcal{D}_t that consists of pairs $(\mathbf{x}_t, \mathbf{y}_t)$, in which $\mathbf{x}_t \in \mathcal{X}$ denotes an input image of size N , and $\mathbf{y}_t \in \mathcal{Y}_t^N$ denotes the corresponding ground-truth (GT) *pixel* labels. The label space $\mathcal{Y}_t = \{c_b\} \cup \mathcal{C}_t$ consists of the current classes in task t , \mathcal{C}_t , and the dummy background class c_b , that is assigned to all pixels that do not belong to \mathcal{C}_t . Thus, the c_b label can be assigned to the objects with the *past* classes $\mathcal{C}^{1:t-1}$, the objects with the *future* classes $\mathcal{C}^{t+1:T}$, or the true background pixels.

After learning task t , the semantic segmentation model f_θ^t is required to predict whether a pixel belongs to *all* the classes learned so far, $\mathcal{C}^{1:t} = \mathcal{C}^{1:t-1} \cup \mathcal{C}_t$, or the true background. As in other work, we assume the classes in each \mathcal{C}_t are disjoint. Typically, the model is defined to be a mapping $f_\theta^t : \mathcal{X} \rightarrow \mathbb{R}^{N \times |\mathcal{Y}^t|}$, in which $\mathcal{Y}^t = \mathcal{C}_d \cup \mathcal{C}^{1:t}$ with \mathcal{C}_d containing dummy labels. All previous work [3, 7] simply set $\mathcal{C}_d = \{c_b\}$, but in our work, we also add the separate “Unknown” class label, c_u , to \mathcal{C}_d , hence, set $\mathcal{C}_d = \{c_b, c_u\}$. Later, we show defining this additional label c_u in our model output plays a critical role in improving the learning capability for future classes. The architecture of f_θ^t is typically a fully-convolutional network, which consists of a convolutional feature extractor, h_ψ^t , followed by the final 1×1 classifier filters, $\{\phi_c^t\}_{c \in \mathcal{Y}^t}$, one for each output class in \mathcal{Y}^t .

The learning of f_θ^t is done in conjunction with the previous model $f_\theta^{t-1} : \mathcal{X} \rightarrow \mathbb{R}^{N \times |\mathcal{Y}^{t-1}|}$ to prevent forgetting during incrementally updating the model. Determining which output classifier (*e.g.*, softmax or sigmoid) to use for each pixel as well as how to transfer the knowledge of f_θ^{t-1} to f_θ^t (*e.g.*, knowledge distillation or model freezing) are design choices, and we elaborate our choices more in details in the subsequent sections. Furthermore, we denote \mathcal{M} as the *exemplar memory*, which can store a small number of samples from past training data, $\mathcal{D}^{1:t-1}$, and use it for learning f_θ^t .

Once the learning of f_θ^t is done, the prediction for pixel i of an input image \mathbf{x} is obtained by

$$\hat{\mathbf{y}}_i^t = \arg \max_{c \in \mathcal{Y}^t} f_{\theta, ic}^t(\mathbf{x}),$$

and the performance is measured by the mean intersection-over-union (mIoU) metric for the classes in \mathcal{Y}^t . (Only in the evaluation phase, we merge c_b and c_u for computing mIoU of the BG class.)

3.2 Two Additional Challenges of CISS

In addition to the typical reason for causing catastrophic forgetting in CIL for classification, *i.e.*, the prediction bias due to the data imbalance, we note there are two additional unique challenges in CISS.

The first challenge, as mentioned in the Introduction and in previous work [3, 7], comes from the semantic drift of the background (BG) label. Namely, the ground-truth label associated with the pixels of the object can change depending on the incremental state. For example, when a pixel is labeled as “BG” at state t , it is possible that the corresponding pixel would be labeled as “sofa” at state $t - 1$ (*i.e.*, past class) or labeled as “dog” at state $t + 1$ (*i.e.*, future class), depending on the true object to which the pixel belongs. Therefore, naively learning with the “BG” target label for the pixel at state t could cause either severe forgetting of the past class (*i.e.*, hurting stability) or interfering the learning of the future class (*i.e.*, hurting plasticity).

The second challenge stems from the fact that semantic segmentation is a multi-label prediction problem. Namely, for a given image, the segmentation model needs to output a *set* of classes, in contrast to the classification model which outputs only a single class. Therefore, the *precision* of the prediction for each pixel becomes important in addition to the recall as is reflected in the mIoU performance metric; *i.e.*, not only predicting a correct class for a pixel is important, but also not predicting a wrong class is important for the overall metric. That is, if the prediction for every pixel

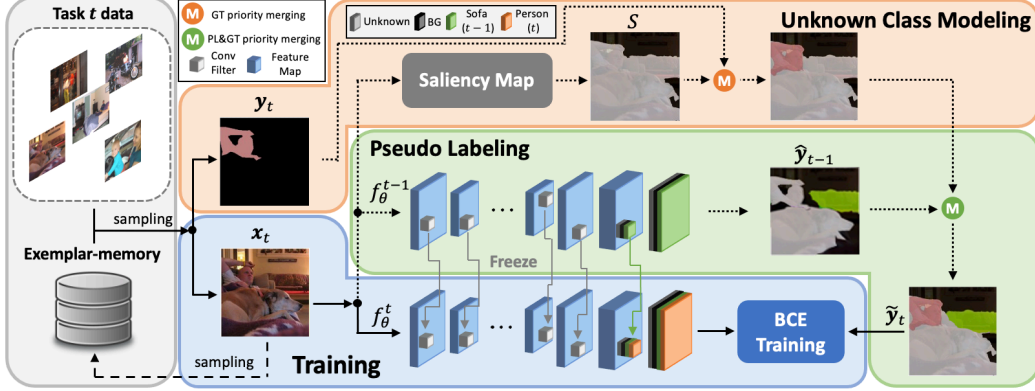


Figure 1: Overall procedure of SSUL. Given $(x_t, y_t) \in \mathcal{D}_t$, the augmented label \tilde{y}_t is first obtained by the “Unknown” class modeling and pseudo-labeling. Then, using \tilde{y}_t as a target, we update f_θ^t with model freezing and BCE loss. The exemplar-memory is also updated with class-balanced sampling.

gets biased toward the current classes in \mathcal{C}_t , the mIoU’s for the past classes in $\mathcal{C}^{1:t-1}$ as well as the current classes would significantly drop jointly. This point is exactly why even the mIoU’s for the newly learned classes are *very low* in [3, 7]. Note this is in a stark difference with the classification, in which the accuracy of the current classes would remain high even with the severe bias and forgetting, since it is a single-label prediction problem.

To address above unique challenges of CISS, we devise our SSUL-M by carefully combining several ideas, of which overall procedure is outlined in Figure 1. We now elaborate on our three main contributions in details: 1) **label augmentation** for BG class with *Unknown* class and pseudo-labels, 2) **stable score learning** with model freeze and sigmoid output, and 3) usage of **tiny exemplar memory** with class-balanced sampling.

3.3 Contribution 1: Label Augmentation for BG Class

Here, we describe how we generate an augmented target label $\tilde{y}_t \in (\mathcal{Y}^t)^N = \{c_b, c_u, \mathcal{C}^{1:t}\}^N$ given a training sample (x_t, y_t) in \mathcal{D}_t . Recall that $y_t \in (\mathcal{Y}_t)^N = \{c_b, \mathcal{C}_t\}^N$.

Unknown class modeling In order to handle the case in which the potential future class objects are labeled as BG, we propose to use a novel unknown class label, c_u , that is defined to designate any foreground objects that are not the current classes in \mathcal{C}_t . Specifically, as depicted in the top part of Figure 1, we first apply an off-the-shelf salient object detector [11] $S : \mathcal{X} \rightarrow \{0, 1\}^N$ to the input image x_t , which assigns 1 to the pixels if they are salient (*i.e.*, part of a foreground object) and 0 otherwise. Then, we assign c_u to the pixels that are BG-labeled but salient; namely, we set $\tilde{y}_{t,i} = c_u$ if $(y_{t,i} = c_b) \wedge (S(x_t)_i = 1)$ for pixel i . In our experiments, we show this Unknown class label plays a critical role so that the base feature extractor can distinguish the representations of the potential future class objects and the true background, even before observing the class labels.

Pseudo-labeling Once augmenting with c_u is done, we further augment with pseudo-labels generated from the previous model f_θ^{t-1} to maintain the knowledge of the past classes, similarly as in [7] and as shown in the middle part of Figure 1. Namely, we denote $\hat{y}_{t-1,i} = \arg \max_{c \in \mathcal{Y}^{t-1}} f_{\theta,ic}^{t-1}(x_t)$ as the prediction of f_θ^{t-1} for the i -th pixel and set $\tilde{y}_{t,i} = \hat{y}_{t-1,i}$ if

$$(y_{t,i} = c_b) \wedge (\hat{y}_{t-1,i} \in \mathcal{C}^{1:t-1}) \wedge (\mu_i > \tau),$$

in which $\mu_i = \max_{c \in \mathcal{C}^{1:t-1}} \sigma(f_{\theta,ic}^{t-1}(x_t))$ stands for the confidence of prediction for $\hat{y}_{t-1,i} \in \mathcal{C}^{1:t-1}$ where $\sigma(\cdot)$ is the sigmoid function, and τ is a threshold (set to 0.7). In words, we assign the pseudo-labels (*i.e.*, the predictions from the previous model) to the pixels that are BG-labeled only when the predictions are made to be the past object classes (excluding c_b and c_u) with enough confidence.

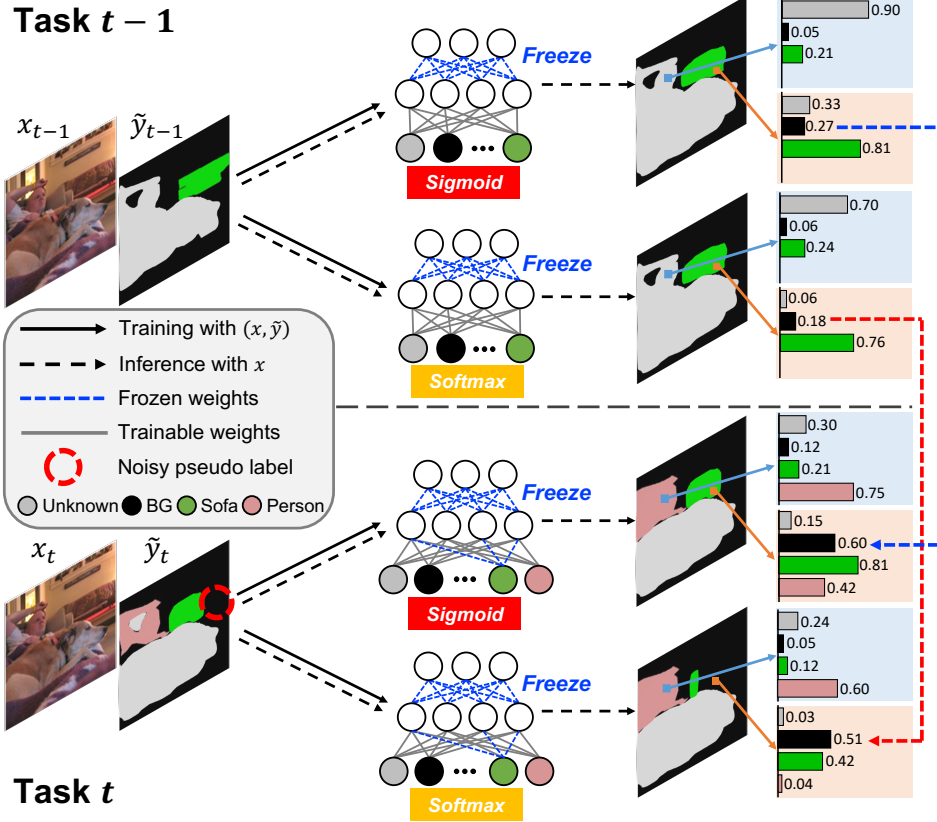


Figure 2: Comparison of the effect on the classification scores for sigmoid with binary cross-entropy (BCE) and softmax with cross-entropy (CE). For a pixel with noisy label $\tilde{y}_{t,i} = c_b$ (i.e., BG label (black) when the true is “sofa” (green), see the red dashed circle at task t), even when the classifier for “sofa” ($\{\phi_c\}_{c \in \mathcal{C}^{1:t-1}}$) is frozen, the softmax would cause the BG class score to rise above the score for “sofa” (see the red dashed arrow), whereas the sigmoid would let the BG score rise only moderately (see the blue dashed arrow). Thus, the classification for the pixel could still become “sofa” for sigmoid, whereas softmax would make a false prediction as BG.

In summary, at the incremental state t , the augmented target label for the i -th pixel becomes

$$\tilde{y}_{t,i} = \begin{cases} \mathbf{y}_{t,i} & \text{if } \mathbf{y}_{t,i} \in \mathcal{C}_t \\ \hat{\mathbf{y}}_{t-1,i} & \text{if } (\mathbf{y}_{t,i} = c_b) \wedge (\hat{\mathbf{y}}_{t-1,i} \in \mathcal{C}^{1:t-1}) \wedge (\mu_i > \tau) \\ c_u & \text{if } (\mathbf{y}_{t,i} = c_b) \wedge (S(\mathbf{x}_t)_i = 1) \wedge \{(\hat{\mathbf{y}}_{t-1,i} \in \mathcal{C}_d) \vee (\mu_i \leq \tau)\} \\ c_b & \text{else,} \end{cases} \quad (1)$$

in which the pseudo-label is generated only for the incremental state $t \geq 2$. Figure 1 shows a concrete example of augmentating \mathbf{y}_t to $\tilde{\mathbf{y}}_t$, in which $\mathcal{C}_{t-1} = \{\text{sofa}\}$ and $\mathcal{C}_t = \{\text{person}\}$.

3.4 Contribution 2: Stable Score Learning

We argue that simply using $\tilde{\mathbf{y}}_t$ as a target and training f_{θ}^t with softmax output layer would make the output scores too unstable as the incremental learning continues. The reason is because the augmented labels are *noisy* and the softmax computes the prediction probability in a *relative* way. As shown in our experiments, such instability significantly hurts the precision of the multi-label prediction. To that end, we propose the following three strategies for the stable learning of output scores.

Model freezing Instead of updating the full model with $\tilde{\mathbf{y}}_t$ at every state t , we *freeze* the convolutional feature extractor, h_{ψ} , after initial learning ($t = 1$) as well as the classifiers for the past classes, $\{\phi_c\}_{c \in \mathcal{C}^{1:t-1}}$, and only learn the 1×1 filters $\phi_{c_b}^t$, $\phi_{c_u}^t$ and $\{\phi_c^t\}_{c \in \mathcal{C}_t}$. Such strict model freezing certainly can prevent forgetting, but is counter-intuitive from the plasticity viewpoint. However, thanks

to the unknown class c_u , it turns out the feature extractor h_ψ can roughly learn the representations for the potential future class objects present with BG label in \mathcal{D}_1 . Thus, it becomes sufficient to learn the decision boundaries for c_b , c_u , and \mathcal{C}_t on those representations at state t .

Sigmoid with binary cross entropy loss For learning $\phi_{c_b}^t$, $\phi_{c_u}^t$ and $\{\phi_c^t\}_{c \in \mathcal{C}_t}$, the choice of output layer and loss function becomes important to make the output score stable. A common choice is the softmax with cross-entropy loss, however, since the target labels for c_b and c_u in $\tilde{\mathbf{y}}_t$ are noisy, we observe the relative scoring of softmax could cause significant forgetting of past classes $\mathcal{C}^{1:t-1}$. To see this, let $s_{ic} = [f_\theta^t(\mathbf{x}_t)]_{ic}$ be the score for class c at pixel i . When the softmax with cross-entropy (CE) is used, the gradient of the loss at s_{ic} becomes $\partial \mathcal{L}_{\text{CE}}^t(\theta) / \partial s_{ic} = \mathbf{p}_{ic} - \mathbb{1}\{c = \tilde{\mathbf{y}}_{t,i}\}$, in which $\mathbf{p}_{ic} = \exp(s_{ic}) / (\sum_{c'} \exp(s_{ic'}))$. The issue occurs when $\tilde{\mathbf{y}}_{t,i} = c_b$ or c_u , while the true label for the pixel should be the past classes in $\mathcal{C}^{1:t-1}$. (Thus, the pseudo-label $\hat{\mathbf{y}}_{t-1,i}$ missed the pixel, which could often happen.) Then, the gradient descent learning will force s_{ic_b} or s_{ic_u} to become much higher than $\{s_{ic}\}_{c \in \mathcal{C}^{1:t-1}}$, the scores obtained from the *frozen* classifiers for past classes. Thus, at test time, for a similarly confusing pixel, the model would tend to predict as c_b or c_u , hence, causing the forgetting of past classes even though their classifiers are fixed.

Therefore, we instead use the sigmoid output with binary cross-entropy (BCE) loss independently for each class. In that case, the gradient of the loss at s_{ic} becomes $\partial \mathcal{L}_{\text{BCE}}^t(\theta) / \partial s_{ic} = \sigma(s_{ic}) - \mathbb{1}\{c = \tilde{\mathbf{y}}_{t,i}\}$, hence, even for above noisy target label case, the scores s_{ic_b} or s_{ic_u} will only increase to a certain absolute level regardless of other class score values, $\{s_{ic}\}_{c \in \mathcal{C}^{1:t-1}}$. Thus, at test time, a similar pixel still may be predicted as a past class in \mathcal{C}^{t-1} since the frozen past classifiers would still output a considerable score — this subtle difference between the loss functions is illustrated in Figure 2.

Weight transfer from unknown class classifier Finally, for learning $\{\phi_c^t\}_{c \in \mathcal{C}_t}$, we initialize all the filters with $\phi_{c_u}^{t-1}$, the classifier learned for the unknown class c_u at the previous state. The reasoning is that the classes in \mathcal{C}_t would have been labeled as c_u (as the potential future classes) in state $t-1$, hence, such weight transfer from $\phi_{c_u}^{t-1}$ would yield stable and fast learning of $\{\phi_c^t\}_{c \in \mathcal{C}_t}$.

3.5 Contribution 3: Tiny Exemplar Memory

Using exemplar-memory to store a small portion of past training data for CIL is backed with a theoretical finding [19] as well as strong empirical results [27, 30, 2, 1, 4] for classification.

Hence, we propose to use it for CISS as well with a tailored *class-balanced* sampling strategy. The main rationale of using the memory is to make sure to include at least one sample with correct GT label per each class in $\mathcal{C}^{1:t-1}$ in the training set for state t .

Namely, even though the pseudo-label $\hat{\mathbf{y}}_{t-1}$ can provide labels for the classes in $\mathcal{C}^{1:t-1}$, it is also possible that the given image \mathbf{x}_t would never contain object cues for $\mathcal{C}^{1:t-1}$. In such a case, even with model freezing and stable score learning, when the confidence for the new class is learned to be high for a pixel (potentially for an old class), the prediction for the pixel could get biased toward the new class, causing the forgetting of the old class. Therefore, by denoting $M = |\mathcal{M}|$, after learning incremental state $t-1$, we sample $M/|\mathcal{C}^{1:t-1}|$ data points from \mathcal{D}_{t-1} , and store them in the memory \mathcal{M} by removing equal number of samples per each class in $\mathcal{C}^{1:t-2}$ from \mathcal{M} . In this way, \mathcal{M} always contains at least one sample from each class in $\mathcal{C}^{1:t-1}$, and we show in the experiments that this class-balanced strategy is more helpful than random sampling [4] as is done for CIL for classification.

Algorithm 1: Pseudo code of SSUL-M

```

1: Require  $f_\theta, \mathcal{M}, T, n_{\text{epochs}}$ , batch size  $K$ 
2:  $f_\theta \leftarrow$  Initialize  $h_\psi, \phi_{c_b}, \phi_{c_u}$ 
3: Initialize  $\mathcal{M}$ 
4: for  $t \leftarrow 1, \dots, T$  do
5:    $f_\theta^t \leftarrow$  Initialize  $\{\phi_c^t\}_{c \in \mathcal{C}_t}$ 
6:   if  $t \neq 1$  then
7:     Freeze  $h_\psi, \{\phi_c^t\}_{c \in \mathcal{C}^{1:t-1}}$ 
8:      $\{\phi_c^t\}_{c \in \mathcal{C}_t} \leftarrow$  Weight Transfer( $\phi_{c_u}^{t-1}$ )
9:   end if
10:  for  $n \leftarrow 1, \dots, n_{\text{epochs}}$  do
11:    for  $B_n \overset{K/2}{\sim} \mathcal{D}_t$  do
12:       $B_{\mathcal{M}} \overset{K/2}{\sim} \mathcal{M}$ 
13:       $\tilde{B}_n, \tilde{B}_{\mathcal{M}} \leftarrow$  Label.Aug. ( $B_n, B_{\mathcal{M}}$ )
14:       $\theta \leftarrow$  SGD( $\tilde{B}_n \cup \tilde{B}_{\mathcal{M}}, \mathcal{L}_{\text{BCE}}^t(\theta)$ )
15:    end for
16:  end for
17:  Update  $\mathcal{M}$ 
18: end for
19: return  $f_\theta^t$ 

```

3.6 Summary

We summarize our SSUL-M algorithm in Algorithm 1, in which our contributions described in Section 3.3~ Section 3.5 are denoted in the typewriter font. Namely, `Label Aug.` stands for generating \tilde{y}_t as in (1) for the selected batches \mathcal{B}_n and $\mathcal{B}_{\mathcal{M}}$, “`Freeze`, `$\mathcal{L}_{\text{BCE}}^t$` , and `Weight Transfer`” denote the methods for the stable score learning described in Section 3.4, and `Update \mathcal{M}` denote the exemplar-memory maintenance with the class balanced sampling as mentioned in Section 3.5. Note we are constructing a mini-batch by sampling equal amount of data from \mathcal{D}_t and \mathcal{M} , hence, the samples in \mathcal{M} act as anchor points to improve the precision of the predictions.

4 Experiments

4.1 Experimental Setting

Dataset We followed the experimental setting of [3] and evaluated our method using Pascal-VOC 2012 [9] and ADE20K [32] datasets. Originally, [3] set two experimental protocols, *disjoint* and *overlapped*, but we believe the latter is more realistic and challenging. Therefore, we evaluated on the *overlapped* setup only. **Pascal VOC 2012** contains 20 foreground object classes and one background class, and **ADE20K** consists of 150 classes of both stuff and objects. We consider several incremental learning scenarios for each dataset, from the scenarios considered by the other baselines to newly proposed *challenging* scenarios with larger number of incremental states. A more detailed description on the datasets is introduced in the Supplementary Material (S.M.).

Evaluation Metrics We use the mean Intersection-over-Union (mIoU) as our evaluation metric, which computes the IoU for each class then computes the average over the classes. The IoU is defined as $\text{IoU} = \text{true-positive} / (\text{true-positive} + \text{false-positive} + \text{false-negative})$.

Implementation Details For all experiments, following other works [7, 3], we use a Deeplabv3 segmentation network [5] with a ResNet-101 [10] backbone pre-trained on ImageNet [6]. We optimize the network using SGD with an initial learning rate of 10^{-2} and a momentum value of 0.9 for all CISS steps. Also, we set the learning rate schedule, data augmentation, and output stride of 16 following [5] for all experiments. For each incremental state t , we train the network for 50 epochs for Pascal VOC with a batch-size of 32 and 60 epochs for ADE20K with a batch-size of 24. We tune the hyperparameters using 20% of the training set as a validation set and report the final results on the standard test set. For the exemplar memory, we utilized memory with a fixed size of $|\mathcal{M}| = 100$ for Pascal VOC and $|\mathcal{M}| = 300$ for ADE20K. To highlight the effect of the exemplar-memory, we report the results of the two versions of our method — SSUL (without memory) and SSUL-M (with memory). For the saliency-map detector to generate the Unknown class label, we employed DSS [11] pretrained on MSRA-B dataset [22], which contains 5,000 labels for salient objects. The experiments were implemented in PyTorch [26] 1.7 with CUDA 10.1 and CuDNN 7 using two NVIDIA V100 GPUs, and all experiments were conducted with NSML [15] framework. More information on the experimental details are in the S.M.

Baselines For a representative of the general regularization-based continual learning method, we select EWC [18] and LWC [20]-MC and applied them to each experimental setup of CISS. For CISS specific baselines, we compared with ILT [24], MiB [3] and PLOP [7], and the Joint Training (Joint) result is also given as an upper bound. Note that PLOP [7] is the current state-of-the-art. We reproduced the results of all baselines using the official code provided by the authors of [7].

4.2 Experimental results on benchmark dataset

Pascal VOC 2012 Following [7, 3], we evaluate our method on four different scenarios, *i.e.*, {10-1, 15-1, 15-5, and 19-1} as well as a more challenging scenario, {5-3}. The numbers in each scenario denote the number of classes to be trained for each state. For example, VOC 5-3 means learning 5 classes at the base task ($t = 1$), and then incrementally learning 3 classes five times (hence, $T = 6$).

In Table 1, we observe our SSUL consistently outperforms the baselines with *huge* margin in all scenarios, even without using the exemplar-memory. Furthermore, the gap widens particularly for more challenging scenarios, namely, for the cases in which the base task has fewer classes and the number of tasks is larger. Note although MiB [3] and PLOP [7] show robustness for simple 2 tasks scenarios (19-1 and 15-5), their performance are *rapidly* dropped in more challenging and practical

Table 1: Experimental results on Pascal VOC 2012.

Method	VOC 10-1 (11 tasks)			VOC 15-1 (6 tasks)			VOC 5-3 (6 tasks)			VOC 19-1 (2 tasks)			VOC 15-5 (2 tasks)		
	0-10	11-20	all	0-15	16-20	all	0-5	6-20	all	0-19	20	all	0-15	16-20	all
EWC [18]	-	-	-	0.30	4.30	1.30	-	-	-	26.90	14.00	26.30	24.30	35.50	27.10
LwF-MC [20]	4.65	5.90	4.95	6.40	8.40	6.90	20.91	36.67	24.66	64.40	13.30	61.90	58.10	35.00	52.30
ILT [24]	7.15	3.67	5.50	8.75	7.99	8.56	22.51	31.66	29.04	67.75	10.88	65.05	67.08	39.23	60.45
MiB [3]	12.25	13.09	12.65	34.22	13.50	29.29	57.10	42.56	46.71	71.43	23.59	69.15	76.37	49.97	70.08
PLOP [7]	44.03	15.51	30.45	65.12	21.11	54.64	17.48	19.16	18.68	75.35	37.35	73.54	75.73	51.71	70.09
SSUL	71.31	45.98	59.25	77.31	36.59	67.61	72.44	50.67	56.89	77.73	29.68	75.44	77.82	50.10	71.22
SSUL-M	74.02	53.23	64.12	78.36	49.01	71.37	71.27	53.21	58.37	77.83	49.76	76.49	78.40	55.80	73.02
Joint	78.41	76.35	77.43	79.77	72.35	77.43	76.91	77.63	77.43	77.51	77.04	77.43	79.77	72.35	77.43

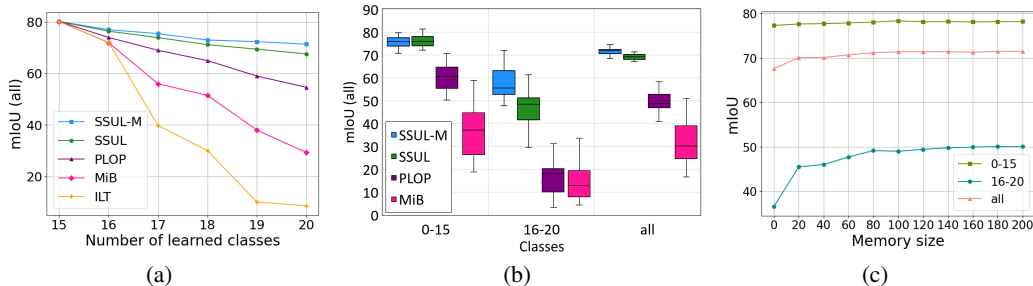


Figure 3: (a): mIoU evaluation on VOC 15-1, (b): mIoU distributions for 20 different class-orderings for VOC 15-1, (c): mIoU on VOC 15-1 with varying memory size $|\mathcal{M}|$.

scenarios (10-1, 5-3, 15-1). More specifically, Figure 3(a) shows the mIoU evolution for 15-1 scenario at each incremental step, and the baselines suffers from a significant drop of mIoU, as the new classes are incrementally learned. In contrast, SSUL improves mIoUs for both base (0-15) and newly learned (16-20) classes significantly, showing much slower drop of mIoU. These results show that as long as the label augmentation of BG class with Unknown class and pseudo-labels is properly done, our stable score learning is very effective for CISS. Particularly, we observe that model freeze, which is believed to be not effective in CIL, is much more effective than the KD used in other baselines.

Furthermore, we observe our SSUL-M, which uses exemplar-memory, further strengthens SSUL significantly, particularly for the newly learned classes (*i.e.*, for $t \geq 2$). For example, in VOC 15-1, by storing only 5 ~ 6 images per class in \mathcal{M} , the mIoU for classes 16-20 improved about 12%. This confirms our intuition that the samples in the memory act as “anchors” to improve the precision of the predictions, hence, prevent forgetting. We can also clearly observe this improvement in Figure 4. As an additional experiment, we also conducted the experiment on the case of further reducing the number of base classes, such as 5-1 and 2-1, and we again observe that our SSUL and SSUL-M surpass other baselines. A detailed result on this additional experiment can be found also in the S.M.

To verify the robustness of each method on various class orderings, we experimented on the 20 difference orderings on VOC 15-1 scenario, as proposed in [7]. Figure 3(b) plots the mIoU distributions for different methods, and we clearly observe both SSUL and SULL-M not only achieve higher mIoUs, but also have smaller variations compared to the baselines. In addition, we note SULL achieves $\times 1.5$ faster training time compared to PLOP due to network freezing.

Qualitative analysis In Figure 4, we visualized the qualitative results for four images from VOC 15-1 task. We observe that PLOP partly maintains knowledge learned from the base task (*bird* and *person*), however, it becomes fatal in forgetting the classes learned in the intermediate steps, such as plant and sheep. In addition, PLOP frequently produces many false-positive predictions, lowering the mIoU of several classes. (E.g., see *bird* in Step 5.) On the other hand, we observe SSUL and SSUL-M both maintains the previously learned classes with high stability and effectively learns new classes. For example, the *sheep* class is accurately learned at Step 3 and not forgotten afterwards. Moreover, we observe SULL-M achieved further improvement of both plasticity and stability over SULL, especially by reducing the false-positive predictions.

ADE20K Unlike VOC 2012, ADE20K is densely labeled for both stuff and thing with 150 classes. It means that the class definition in ADE20K is clearer therefore, it naturally make reduce the concern about the semantic drift of BG label. To make efficient use of this prior knowledge of dataset, we

Table 2: Experimental results on ADE20K.

Method	ADE 100-5 (11 tasks)			ADE 100-10 (6 tasks)			ADE 100-50 (2 tasks)			ADE 50-50 (3 tasks)		
	0-100	101-150	all	0-100	101-150	all	0-100	101-150	all	0-50	511-150	all
ILT [24]	0.08	1.31	0.49	0.11	3.06	1.09	18.29	14.40	17.00	3.53	12.85	9.70
MiB [3]	36.01	5.66	25.96	38.21	11.12	29.24	40.52	17.17	32.79	45.57	21.01	29.31
PLOP [7]	39.11	7.81	28.75	40.48	13.61	31.59	41.87	14.89	32.94	48.83	20.99	30.40
SSUL	39.94	17.40	32.48	40.20	18.75	33.10	41.28	18.02	33.58	48.38	20.15	29.56
SSUL-M	42.86	17.78	34.56	42.86	17.66	34.46	42.79	17.54	34.37	49.12	20.10	29.77
Joint	44.30	28.20	38.90	44.30	28.20	38.90	44.30	28.20	38.90	51.10	33.30	38.90

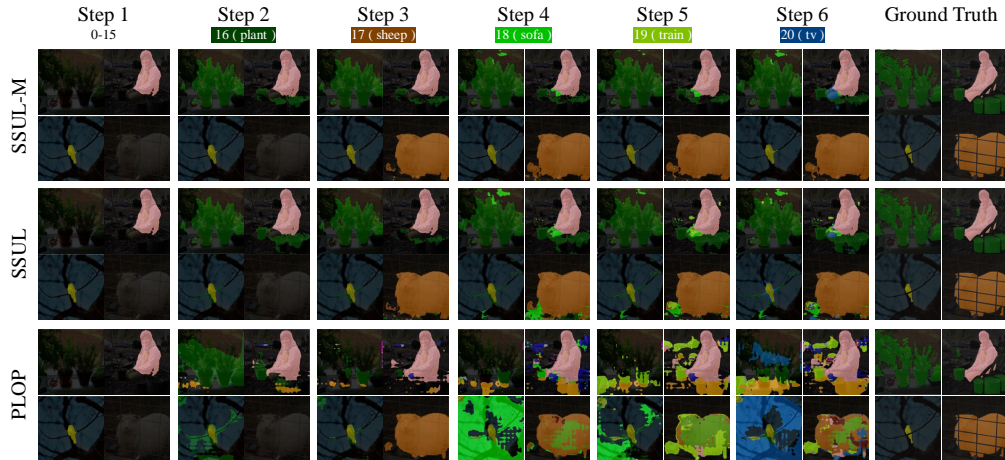


Figure 4: Qualitative results of SSUL-M, SSUL and PLOP on VOC 15-1 scenario.

consider unlabeled pixels as unknown class without using the saliency detector and enlarge the size of memory to $|\mathcal{M}| = 300$. We evaluated our method in four different scenarios, *i.e.*, $\{100-5, 100-10, 50-50, 100-50\}$ as in [7, 3]. Table 2 again shows that SSUL achieves superior performance in the more challenging tasks (100-5, 100-10) than other methods. We believe that, this result demonstrates SSUL is also quite effective in CISS for a densely labeled dataset, without any extra saliency detector. The qualitative analysis on ADE20K is provided in the S.M.

4.3 Ablation Study

Ablation study on proposed components of SSUL Here, we analyze the effect of each proposed component of SSUL on VOC 15-1 scenario. Table 3 compares the mIoU of each ablation case, without memory, and the first low shows the result of SSUL with full components. Firstly, when the Unknown class is removed, we clearly observe that the mIoU's of both the first task (0-15) and subsequent classes (16-20) decrease. Hence, this clearly demonstrates the advantage of using the Unknown class label, in terms of increasing both the plasticity and stability. Secondly, note that model freezing has a significant impact on the performance of CISS. Specifically, it not only prevents catastrophic forgetting on the first task, but also plays a critical role to learn new classes well. Finally, we observe when Softmax+CE instead of Sigmoid+BCE is used (the last ablation), the forgetting of the first task (0-15) drops more significantly despite model freezing. We believe this confirms our intuition in Section 3.4 on why Sigmoid+BCE can lead to more stable score learning.

Saliency-map detector and weight transfer The first two columns in Table 4 shows the ablation study on saliency-map detector for Unknown class and weight transfer. We compare the result of a default neural network-based saliency map extractor, DSS [11] with ground-truth and a random forest-based DRFI [13]. We observe the differences of the mIoU's among them are quite small, therefore, we believe that the quality of saliency map is not a significant factor of our method. The ablation study on weight transfer demonstrates weights for new classes initialized with $\phi_{c_u}^{t-1}$ is most effective to learn it. This result may at first look counter-intuitive since learning the final linear layer ϕ_c^t should not be sensitive on the initialization. However, given the *noisy* pseudo-label for learning, a quicker convergence of ϕ_c^t using the warm-start weight $\phi_{c_u}^{t-1}$ would effectively prevent the forgetting of past class, which could be caused by fitting the noisy pseudo-label for many epochs. More details on the effect of weight transfer is proposed in S.M.

Table 3: Ablation study for SSUL on VOC 15-1 about PL (pseudo labeling), Unknown (unknown class modeling & weight transfer), Freeze (model freezing), and Sigmoid+BCE (stable score learning).

	PL	Unknown	Freeze	Sigmoid+BCE	15-1 (6 tasks)		
					0-15	16-20	all
	✓	✓	✓	✓	77.31	36.59	67.61
	✓	✗	✓	✓	73.42	21.79	61.12
	✓	✓	✗	✓	53.56	14.48	44.25
	✓	✓	✓	✗	61.42	22.97	52.26

Table 4: Ablation study for saliency-map detector (left), weight transfer (mid), and memory sampling (right) on VOC 15-1.

Saliency-map detector				Weight transfer				Memory sampling			
Methods	0-15	16-20	all	Methods	0-15	16-20	all	Methods	0-15	16-20	all
DRFI [13]	76.46	32.53	66.00	$random \rightarrow \phi_c^t$	73.73	23.99	61.89	random	78.61	38.87	69.15
DSS [11]	77.31	36.59	67.61	$\phi_{c_b}^{t-1} \rightarrow \phi_c^t$	73.29	23.70	61.48	class-balanced	78.36	49.01	71.37
ground-truth	78.42	40.41	69.36	$\phi_{c_u}^{t-1} \rightarrow \phi_c^t$	77.31	36.59	67.61	-	-	-	-

Memory size and sampling rule The right column row of Table 4 shows the result of the mIoU on two sampling rules. We observe that, compared to random sampling, our proposed class-balanced sampling achieves better mIoU, particularly for the newly learned classes. We believe the reason is class-balanced sampling ensures at least one sample per class, therefore, it prevents the forgetting of minority classes than random sampling, which can miss certain classes in \mathcal{M} . Finally, Figure 3(c) shows the dependency of SSUL-M on the memory size. It illustrates that tiny exemplar-memory for CISS significantly helps to increase the mIoU for the newly learned classes (16-20) than the base classes (0-15). Moreover, we observe that after sufficiently large $|\mathcal{M}|$ the mIoU performance becomes robust.

5 Concluding Remarks and Limitation

We proposed a new class-incremental learning method SSUL-M (Semantic Segmentation with Unknown Label with Memory) for semantic segmentation. In order to address two additional challenges of CISS, we made three main contributions — label augmentation with Unknown class labels, stable score learning, and tiny exemplar memory. They all were convincingly shown to be very effective in various CISS scenarios and our SSUL-M significantly outperformed baselines.

While promising, we admit our work also has some limitations as follows. First, our unknown class modeling may not be satisfactory for some “stuff” segmentation tasks since saliency-maps are mainly targeted for “things” (or objects). Second, our model freezing may harm plasticity and cause the model suffer from learning new classes especially when they are not captured by the unknown class label during the base task. Together with our insights from the analyses of SULL-M, we believe attempting to address above limitations would lead to a fruitful future research directions for the CISS problem.

Acknowledgement

This work was done while Sungmin Cha did a research internship at NAVER AI Lab. This work was supported in part by the New Faculty Startup Fund from Seoul National University, NRF Mid-Career Research Program [NRF-2021R1A2C2007884] funded by the Korean government, and SNU-NAVER Hyperscale AI Center. The authors thank NAVER Smart Machine Learning (NSML) team for the GPU support. Taesup Moon also thanks the support from Automation and Systems Research Institute (ASRI) at Seoul National University.

References

- [1] Hongjoon Ahn, Jihwan Kwak, Subin Lim, Hyeonsu Bang, Hyojun Kim, and Taesup Moon. Ss-il: Separated softmax for incremental learning. *arXiv preprint arXiv:2003.13947*, 2020.
- [2] Francisco M Castro, Manuel J Marín-Jiménez, Nicolás Guil, Cordelia Schmid, and Karteek Alahari. End-to-end incremental learning. In *Proceedings of the European conference on computer vision (ECCV)*, pages 233–248, 2018.
- [3] Fabio Cermelli, Massimiliano Mancini, Samuel Rota Buló, Elisa Ricci, and Barbara Caputo. Modeling the background for incremental learning in semantic segmentation. In *Proceedings of the IEEE/CVF Conference on Computer Vision and Pattern Recognition*, pages 9233–9242, 2020.
- [4] Arslan Chaudhry, Marcus Rohrbach, Mohamed Elhoseiny, Thalaiyasingam Ajanthan, Puneet K Dokania, Philip HS Torr, and Marc’Aurelio Ranzato. On tiny episodic memories in continual learning. *arXiv preprint arXiv:1902.10486*, 2019.
- [5] Liang-Chieh Chen, George Papandreou, Florian Schroff, and Hartwig Adam. Rethinking atrous convolution for semantic image segmentation. *arXiv preprint arXiv:1706.05587*, 2017.
- [6] Jia Deng, Wei Dong, Richard Socher, Li-Jia Li, Kai Li, and Li Fei-Fei. Imagenet: A large-scale hierarchical image database. In *2009 IEEE conference on computer vision and pattern recognition*, pages 248–255. Ieee, 2009.
- [7] Arthur Douillard, Yifu Chen, Arnaud Dapogny, and Matthieu Cord. Plop: Learning without forgetting for continual semantic segmentation. *arXiv preprint arXiv:2011.11390*, 2020.
- [8] Arthur Douillard, Matthieu Cord, Charles Ollion, Thomas Robert, and Eduardo Valle. Podnet: Pooled outputs distillation for small-tasks incremental learning. In *Computer vision-ECCV 2020-16th European conference, Glasgow, UK, August 23-28, 2020, Proceedings, Part XX*, volume 12365, pages 86–102. Springer, 2020.
- [9] Mark Everingham, Luc Van Gool, Christopher KI Williams, John Winn, and Andrew Zisserman. The pascal visual object classes (voc) challenge. *International journal of computer vision*, 88(2):303–338, 2010.
- [10] Kaiming He, Xiangyu Zhang, Shaoqing Ren, and Jian Sun. Deep residual learning for image recognition. In *Proceedings of the IEEE conference on computer vision and pattern recognition*, pages 770–778, 2016.
- [11] Qibin Hou, Ming-Ming Cheng, Xiaowei Hu, Ali Borji, Zhuowen Tu, and Philip HS Torr. Deeply supervised salient object detection with short connections. In *Proceedings of the IEEE conference on computer vision and pattern recognition*, pages 3203–3212, 2017.
- [12] Saihui Hou, Xinyu Pan, Chen Change Loy, Zilei Wang, and Dahua Lin. Learning a unified classifier incrementally via rebalancing. In *Proceedings of the IEEE/CVF Conference on Computer Vision and Pattern Recognition*, pages 831–839, 2019.
- [13] Huaizu Jiang, Jingdong Wang, Zejian Yuan, Yang Wu, Nanning Zheng, and Shipeng Li. Salient object detection: A discriminative regional feature integration approach. In *Proceedings of the IEEE conference on computer vision and pattern recognition*, pages 2083–2090, 2013.
- [14] Beomyoung Kim, Sangeun Han, and Junmo Kim. Discriminative region suppression for weakly-supervised semantic segmentation. In *Proceedings of the AAAI Conference on Artificial Intelligence*, volume 35, pages 1754–1761, 2021.
- [15] Hanjoo Kim, Minkyu Kim, Dongjoo Seo, Jinwoong Kim, Heungseok Park, Soeun Park, Hyunwoo Jo, KyungHyun Kim, Youngil Yang, Youngkwan Kim, et al. Nsm1: Meet the mlaas platform with a real-world case study. *arXiv preprint arXiv:1810.09957*, 2018.
- [16] Jang-Hyun Kim, Wonho Choo, and Hyun Oh Song. Puzzle mix: Exploiting saliency and local statistics for optimal mixup. In *International Conference on Machine Learning*, pages 5275–5285. PMLR, 2020.
- [17] JangHyun Kim, Wonho Choo, Hosan Jeong, and Hyun Oh Song. Co-mixup: Saliency guided joint mixup with supermodular diversity. In *International Conference on Learning Representations*, 2021.
- [18] James Kirkpatrick, Razvan Pascanu, Neil Rabinowitz, Joel Veness, Guillaume Desjardins, Andrei A. Rusu, Kieran Milan, John Quan, Tiago Ramalho, Agnieszka Grabska-Barwinska, Demis Hassabis, Claudia Clopath, Dharshan Kumaran, and Raia Hadsell. Overcoming catastrophic forgetting in neural networks. *Proceedings of the National Academy of Sciences*, 114(13):3521–3526, 2017.

- [19] Jeremias Knoblauch, Hisham Husain, and Tom Diethe. Optimal continual learning has perfect memory and is np-hard. In *International Conference on Machine Learning*, pages 5327–5337. PMLR, 2020.
- [20] Zhizhong Li and Derek Hoiem. Learning without forgetting. *IEEE Transactions on Pattern Analysis and Machine Intelligence*, 40(12):2935–2947, 2017.
- [21] Jiang-Jiang Liu, Qibin Hou, Ming-Ming Cheng, Jiashi Feng, and Jianmin Jiang. A simple pooling-based design for real-time salient object detection. In *Proceedings of the IEEE/CVF Conference on Computer Vision and Pattern Recognition*, pages 3917–3926, 2019.
- [22] Tie Liu, Zejian Yuan, Jian Sun, Jingdong Wang, Nanning Zheng, Xiaoou Tang, and Heung-Yeung Shum. Learning to detect a salient object. *IEEE Transactions on Pattern analysis and machine intelligence*, 33(2):353–367, 2010.
- [23] Michael McCloskey and Neal J Cohen. Catastrophic interference in connectionist networks: The sequential learning problem. In *Psychology of learning and motivation*, volume 24, pages 109–165. Elsevier, 1989.
- [24] Umberto Michieli and Pietro Zanuttigh. Incremental learning techniques for semantic segmentation. In *Proceedings of the IEEE/CVF International Conference on Computer Vision Workshops*, pages 0–0, 2019.
- [25] German I Parisi, Ronald Kemker, Jose L Part, Christopher Kanan, and Stefan Wermter. Continual lifelong learning with neural networks: A review. *Neural Networks*, 113:54–71, 2019.
- [26] Adam Paszke, Sam Gross, Francisco Massa, Adam Lerer, James Bradbury, Gregory Chanan, Trevor Killeen, Zeming Lin, Natalia Gimelshein, Luca Antiga, et al. Pytorch: An imperative style, high-performance deep learning library. *Advances in neural information processing systems*, 32:8026–8037, 2019.
- [27] Sylvestre-Alvise Rebuffi, Alexander Kolesnikov, Georg Sperl, and Christoph H Lampert. icarl: Incremental classifier and representation learning. In *Proceedings of the IEEE conference on Computer Vision and Pattern Recognition (CVPR)*, pages 2001–2010, 2017.
- [28] Gido M Van de Ven and Andreas S Tolias. Three scenarios for continual learning. *arXiv preprint arXiv:1904.07734*, 2019.
- [29] Yunchao Wei, Jiashi Feng, Xiaodan Liang, Ming-Ming Cheng, Yao Zhao, and Shuicheng Yan. Object region mining with adversarial erasing: A simple classification to semantic segmentation approach. In *Proceedings of the IEEE conference on computer vision and pattern recognition*, pages 1568–1576, 2017.
- [30] Yue Wu, Yinpeng Chen, Lijuan Wang, Yuancheng Ye, Zicheng Liu, Yandong Guo, and Yun Fu. Large scale incremental learning. In *Proceedings of the IEEE/CVF Conference on Computer Vision and Pattern Recognition*, pages 374–382, 2019.
- [31] Qi Yao and Xiaojin Gong. Saliency guided self-attention network for weakly and semi-supervised semantic segmentation. *IEEE Access*, 8:14413–14423, 2020.
- [32] Bolei Zhou, Hang Zhao, Xavier Puig, Sanja Fidler, Adela Barriuso, and Antonio Torralba. Scene parsing through ade20k dataset. In *Proceedings of the IEEE conference on computer vision and pattern recognition*, pages 633–641, 2017.

Supplementary Materials for SSUL: Semantic Segmentation with Unknown Label for Exemplar-based Class-Incremental Learning

Sungmin Cha^{1,2*}, Beomyoung Kim^{3*}, Youngjoon Yoo^{2,3}, and Taesup Moon¹

¹ Department of Electrical and Computer Engineering, Seoul National University

² NAVER AI Lab, ³ Face, NAVER Clova

sungmin.cha@snu.ac.kr, {beomyoung.kim, youngjoon.yoo}@navercorp.com,
tsmoon@snu.ac.kr

1 Additional Discussions

1.1 On model freezing and plasticity

The model freezing may seem too restrictive as it may focus too much on maintaining the performance of the old classes and limit the capability of learning new classes. However, in our ablation study (Table 3 in the manuscript), by comparing 1st and 3rd line of the table, we observe that model freezing significantly improves the mIoU not only for the old classes, but also for the new classes. This somewhat counterintuitive phenomenon mainly has to do with the second challenge mentioned above — *i.e.*, since the predictions for the old classes remain accurate, the mIoU for the new classes also improves by limiting the false positives.

With such a positive effect of model freezing on the mIoU for the new classes, the unknown class label is introduced to compensate for the restrictiveness of complete freezing of the feature extractor in learning new classes and deal with the BG shift issue. Comparing the 1st and 2nd line of Table 3 in the manuscript shows that the unknown class clearly further improves the performance for the new classes by effectively learning the representations of potential future classes (embedded in the unknown class). Note the result of SSUL (for VOC 15-1 task) is better than that of PLOP not only for the old classes, but also for the new classes when the unknown class label is used.

Finally, the learning capability for the new classes significantly gets boosted with the usage of the exemplar-memory. That is, for the VOC 15-1 task in Table 1, the mIoU for the new classes improves from 36.59% (SSUL) to 49.01% (SSUL-M). This again is due to the fact that the ground-truth labels for the old classes in the memory help make less false positive errors for the new classes.

In summary, although the model freezing may seem somewhat counterintuitive for achieving the plasticity, we convincingly show that it is very effective not only for maintaining the performance of the old classes, but also for learning the new classes in the CISS problem.

1.2 The case for stuff (area-like) and thing (object-like) classes in CISS

One of our main target issues is the semantic drift between true background and future class, and we alleviate the issue using the unknown class modeling with saliency maps. We believe that the applicability of the saliency maps depends on the dataset condition, that is, the matter is how many true backgrounds are included in the dataset.

Firstly, the segmentation datasets including only the object/thing (e.g., Pascal VOC) contain a huge number of true backgrounds. In this case, we showed that our unknown modeling with saliency maps

*Equal contribution.

is greatly helpful to alleviate the semantic drift between true background and future class (in Table 1, Figure 3 and Figure 4 of the manuscript). Secondly, if the segmentation dataset including both the thing and stuff contains few true background pixels (e.g., ADE20K), the semantic drift rarely occurs. In this case, we can apply our unknown modeling without saliency maps and achieve a reasonable performance as in Table 2 of the manuscript. Finally, if the segmentation dataset including the thing and stuff contains many true backgrounds, the saliency maps may not be helpful.

Nevertheless, we respectfully argue that the final case, that is, the dataset supports stuff segmentation yet contains many true backgrounds is not a common condition. Most famous datasets (e.g., Cityscape [4], COCO-stuff [2], Pascal Context [10], and NYU [11]) contain few true backgrounds, therefore, our unknown modeling can widely be utilized in the same way as applied to ADE20K.

1.3 The details on sampling strategy for tiny exemplar memory

Here, we describe the details of exemplar memory sampling strategy. We denoted that the exemplar memory as \mathcal{M} and the size of exemplar memory as $M = |\mathcal{M}|$. After learning the incremental step $t - 1$ ($t > 0$), we sample the \mathcal{M} for $\mathcal{C}^{1:t-1}$ in \mathcal{D}_{t-1} . For the *random* sampling strategy, we randomly select the data from \mathcal{D}_{t-1} until the size of \mathcal{M} becomes M . However, as mentioned in the ablation study section of the main paper, majority classes (e.g., person, dog, car) are mainly sampled in \mathcal{M} , and none of the minority classes (e.g., TV, plant) may be sampled in \mathcal{M} , inducing the catastrophic forgetting of the minority classes. To alleviate the problem, we designed the *class-balanced* sampling strategy; for each class in $\mathcal{C}^{1:t-1}$, we collect $M/|\mathcal{C}^{1:t-1}|$ samples in \mathcal{D}_{t-1} and store them in the \mathcal{M} . When the $|\mathcal{M}|$ is not equal to M , we randomly drop or supplement the samples in \mathcal{M} until $|\mathcal{M}| = M$. In addition, at the $t + 1$ step, we remove some samples of each class (i.e., $\mathcal{C}^{1:t-1}$) in \mathcal{M} and add samples for \mathcal{C}_t to \mathcal{M} , so that \mathcal{M} contains $M/|\mathcal{C}^{1:t}|$ samples per each class. This strategy ensures that \mathcal{M} always contains at least one sample for each class, and we verified that the effectiveness of the *class-balanced* sampling strategy in the Table 4 of the manuscript.

2 Additional Details of Datasets

Pascal VOC 2012 consists of 13,487 images, and it is divided as 10,582 images for training, 1,449 images for validation and 1,456 images for test dataset. **ADE20K** is a large scale dataset for semantic segmentation of scenes, including 25,210 images. It is also grouped as 20,210 images for the training set, 2,000 images for the validation set, and 3,000 images for the testing set. As stated in the manuscript, we followed exactly same experimental settings with PLOP [5].

3 The More Details of Experiments on Pascal VOC 2012

3.1 The experimental result on reducing the initial number of classes

The result for the case in which the initial class set is small can be found in Table 1 (VOC 5-3 task) in the manuscript, and we observe our method still significantly surpasses the baselines. Furthermore, we carried out additional experiments with small initial classes (i.e., VOC 5-1, 2-1, and 2-2 tasks), as shown in Table 1. We again observe that our SSUL consistently outperforms other baselines by a large margin even for such extreme cases, which confirms the effectiveness of our SSUL method.

Table 1: The experiment result on the small initial number of classes.

Method	VOC 10-1 (11 tasks)			VOC 5-1 (16 tasks)			VOC 2-1 (19 tasks)			VOC 2-2 (10 tasks)		
	0-10	11-20	all	0-5	6-20	all	0-2	3-20	all	0-2	3-20	all
MiB [3]	12.25	13.09	12.65	11.47	9.45	10.03	21.57	7.93	9.88	41.11	23.35	25.89
PLOP [5]	44.03	15.51	30.45	0.12	9.00	6.46	0.01	5.22	4.47	24.05	11.92	13.66
SSUL	71.31	45.98	59.25	69.32	40.38	48.65	62.35	34.32	38.32	62.38	42.46	45.31
SSUL-M	74.02	53.23	64.12	71.86	48.41	55.11	60.49	42.11	44.74	58.85	45.82	47.68

3.2 The additional ablation study on weight transfer

One may think the initialization of the final linear layer would not matter since the feature extractor is frozen. However, as also observed in prior work on CIL [1, 6], the number of training iterations or the level of overfitting during learning seems to play an important role in finding the right trade-off between learning new classes and not forgetting the old classes. To that regard, we did additional experiments checking the effect of initialization and the number of training iterations in Table 2. Namely, we simply did the random initialization for ϕ_c^t and increased the number of iterations ($\times 1$, $\times 2$, $\times 4$) and compared with our weight transfer ($\times 1$) results. From the table, we observe that the random initialization cannot reach the performance of weight transfer even with a larger number of iterations. We argue this is a similar phenomenon as what we observe in ordinary CIL. Namely, for the new class sigmoid, it is true that the linear weight would converge to the same solution regardless of the initialization. However, the number of iterations to reach the solution would differ – if we do the weight transfer, it will converge quicker, whereas if randomly initialized, a larger epoch would be necessary. Now, in the latter case, running with a larger epoch would result in the overfitting of the weights for c_u and c_b to the noisy pseudo label. Then, it will cause overconfident predictions for the Unknown or Background classes, which would penalize the overall mIoU. On the other hand, when only a small number of iterations are used for the random initialization, the prediction for the new class would become inaccurate, which again would hurt the overall mIoU.

Table 2: The additional ablation study for weight transfer

Head Init	Iterations	VOC 15-1 (6 tasks)		
		0-15	16-20	all
Random	$\times 1$	73.73	23.99	61.89
Random	$\times 2$	73.89	23.08	62.45
Random	$\times 4$	72.22	22.38	61.14
Weight Transfer	$\times 1$	77.31	36.59	67.61

3.3 The effect of using the saliency-detector

In order to observe the effect of using the saliency-detector on the performance of other baselines, we additionally experimented with a variant of PLOP. That is, we implemented PLOP with saliency map, which only used the pseudo-labels that exist in the salient regions, similarly as in ours. As we can see in Table 3, PLOP with saliency map slightly improves the original PLOP by 2.37% (*i.e.*, 54.64% \rightarrow 57.01%). However, such result is still significantly lower than the result of SSUL (67.61%), underscoring the fact that our gain is not merely stemming from the additional data required for training the saliency detector.

Furthermore, even in our SSUL, we note that just naively using the saliency map would not automatically bring the mIoU gain. Namely, the saliency detector is closely used with our unknown class modeling, however, as we can see in Table 3 (2nd line) and Table 4 (weight transfer column) in the manuscript, if the correct weight transfer is not used, the mIoU becomes 61.89% even with the unknown class, which is not much higher than the result without the saliency detector and unknown class, *i.e.*, 61.12%. Note we can enjoy the improvement to 67.61% (+6.49%) only when the proper weight transfer is applied.

Table 3: The additional experiments using the saliency-detector.

	Saliency	VOC 15-1 (6 tasks)		
		0-15	16-20	all
PLOP	\times	65.12	21.11	54.64
PLOP	\checkmark	67.25	24.22	57.01
SSUL	\checkmark	77.31	36.59	67.61

3.4 Additional hyperparameter search for τ

When we generate the pseudo-label, we set the threshold τ on the output of previous model $\mu_i = \max_{c \in \mathcal{C}^{1:t-1}} \sigma(f_{\theta, ic}^{t-1}(\mathbf{x}_t))$ for the confident pseudo-label. Here, we conduct an experiment to analyze

the effect of the hyperparameter τ in Table 4. When $\tau = 0$, which means without the thresholding, we can still achieve a competitive performance of 67.44% all mIoU, however, we found that some noisy labels are included in the pseudo-label. To increase the confidence of the pseudo-label and reduce the noisy labels, we set the τ and found that enough high τ of 0.7 can slightly boost the performance. In addition, as in Table 4, we found that the proposed method is robust to the τ .

Table 4: Effect of threshold τ .

τ	VOC 15-1 (6 tasks)		
	0-15	16-20	all
0.0	77.31	35.85	67.44
0.3	77.51	36.06	67.64
0.5	77.34	35.96	67.49
0.7	77.28	37.51	67.81
0.9	77.31	36.59	67.61
1.0	75.08	40.08	66.74

3.5 The experimental result on disjoint setup

As mentioned in seminar works [3, 5], the disjoint setup has an additional constraint that only the classes observed so far are present in the input image, which is not necessarily practical. However, in this section, we provide an additional experiment result on the disjoint setup on Table 5. We clearly observe that SSUL and SSUL-M again achieve superior results compared to other baselines.

Table 5: Experimental results on Pascal VOC 2012 for *disjoint* setup.

Method	VOC 10-1 (11 tasks)			VOC 15-1 (6 tasks)			VOC 19-1 (2 tasks)			VOC 15-5 (2 tasks)		
	0-10	11-20	all	0-15	16-20	all	0-19	20	all	0-15	16-20	all
EWC [7]	-	-	-	0.30	4.30	1.30	23.20	16.00	22.90	26.70	37.70	29.40
LwF-MC [8]	-	-	-	4.50	7.00	5.20	63.00	13.20	60.50	67.20	41.20	60.70
ILT [9]	-	-	-	3.70	5.70	4.20	69.10	16.40	66.40	63.20	39.50	57.30
MiB [3]	-	-	-	46.20	12.90	37.90	69.60	25.60	67.40	71.80	43.30	64.70
PLOP [5]	-	-	-	57.86	13.67	46.48	75.37	38.89	73.64	71.00	42.82	64.29
SSUL	65.39	34.90	50.87	73.97	32.15	64.01	77.38	22.43	74.76	76.44	45.60	69.10
SSUL-M	65.02	40.82	53.50	76.46	43.37	68.58	77.58	43.89	75.98	76.47	48.55	69.83
Joint	78.41	76.35	77.43	79.77	72.35	77.43	77.51	77.04	77.43	79.77	72.35	77.43

3.6 The details of experimental results of Pascal VOC 2012

Table 6 shows the summarized results of Pascal VOC 2012 by each class.

Table 6: Details of Pascal VOC 2012 mIoU performance per class.

	bg	aero	bike	bird	boat	bottle	bus	car	cat	chair	cow	table	dog	horse	mbike	person	plant	sheep	sofa	train	tv	mIoU	
10-1 (11 tasks)																							
SSUL	88.55	84.42	36.93	84.63	67.40	80.16	76.53	88.01	87.88	34.38	55.55	27.08	69.92	41.33	63.27	80.73	26.89	39.38	26.43	46.10	38.69	59.25	
SSUL-M	88.19	85.98	37.57	86.14	67.85	75.67	90.55	86.25	86.89	35.07	74.09	35.01	71.88	51.85	70.50	80.82	28.90	54.51	26.67	65.56	46.65	64.12	
15-1 (6 tasks)																							
SSUL	89.55	88.99	41.01	88.37	69.45	80.82	85.55	88.47	92.55	35.52	77.02	56.74	90.11	83.46	84.30	85.12	32.98	49.63	26.60	43.38	30.39	67.61	
SSUL-M	90.83	89.78	40.26	89.79	71.44	79.53	93.44	87.16	92.84	35.43	83.86	55.51	89.85	83.63	85.36	85.03	31.76	63.90	29.97	69.29	50.15	71.37	
5-3 (6 tasks)																							
SSUL	86.49	73.10	37.84	85.10	65.05	79.49	41.21	59.68	67.67	12.58	43.94	37.13	61.67	35.69	61.22	78.54	35.61	46.74	21.00	34.18	43.85	52.75	
SSUL-M	88.35	80.21	37.13	84.98	66.68	80.12	58.45	64.79	66.72	14.45	48.51	38.88	61.87	33.32	65.88	77.90	33.54	46.96	24.77	50.02	49.31	55.85	
19-1 (2 tasks)																							
SSUL	92.24	88.93	40.47	89.59	70.85	79.60	95.08	88.61	93.68	37.25	84.78	59.76	89.52	85.88	87.57	84.61	61.33	82.25	54.50	88.14	29.68	75.44	
SSUL-M	92.94	89.93	40.21	89.66	73.80	80.31	93.36	88.13	92.76	37.16	87.85	58.60	88.94	87.05	85.59	85.16	60.82	83.87	55.09	85.44	49.76	76.49	
15-5 (2 tasks)																							
SSUL	91.54	89.80	40.01	88.59	70.28	81.18	89.66	88.02	92.81	36.78	75.70	56.69	90.00	83.56	85.17	85.42	36.03	57.74	32.08	70.09	54.57	71.22	
SSUL-M	91.68	89.33	40.16	88.62	70.95	80.39	93.94	86.66	92.98	36.73	84.50	55.34	89.83	83.15	84.99	85.16	38.93	71.38	35.43	75.95	57.35	73.02	

3.7 The details of experimental results of class orderings

Table 7 shows the numerical details for SSUL and SSUL-M of Figure 3(b) in the manuscript. Note that we strictly followed the class orderings of Pascal VOC 2012 as done in PLOP [5]:

Table 7: Details of the performances for each class ordering on VOC 15-1 scenario.

15-1 (6 tasks)	Class Ordering																			
	1	2	3	4	5	6	7	8	9	10	11	12	13	14	15	16	17	18	19	20
SSUL																				
0-15	77.31	75.48	72.82	76.45	77.13	72.39	76.66	81.43	74.61	73.98	77.41	79.76	78.42	78.47	73.66	78.42	75.11	74.36	74.29	72.19
16-20	36.59	51.37	53.69	54.70	47.08	50.99	40.70	29.67	49.09	47.94	38.89	44.86	49.07	40.22	50.90	44.75	50.34	55.24	47.65	61.40
all	67.61	69.74	68.26	71.27	69.98	67.29	68.10	69.10	68.53	67.78	68.24	71.45	71.44	69.37	68.24	70.41	69.21	69.81	67.95	69.62
SSUL-M																				
0-15	78.36	75.44	73.01	76.42	77.12	72.75	77.17	77.41	74.85	73.68	77.41	79.83	77.66	78.87	74.72	78.27	75.61	74.65	72.81	70.85
16-20	49.01	53.99	72.01	68.77	58.78	65.58	55.74	52.88	57.09	55.45	52.88	48.33	55.13	50.22	64.42	54.00	63.46	62.55	47.93	61.27
all	71.37	70.33	72.77	74.60	72.75	71.01	72.07	71.57	70.62	69.34	71.57	72.33	72.29	72.05	72.27	72.49	72.72	71.77	66.89	68.57

4 Qualitative analysis on ADE20K

In Figure 1, we visualized the qualitative results from ADE20K 100-10 (6 tasks) scenario. We argue that we seldom suffer from the background semantic shift issue on ADE20K because its clear and dense labels for both things and stuff. Consequently, the false-positive predictions are noticeably reduced compared to the results on Pascal VOC 2012. As in Figure 1, the *unknown* label (*i.e.*, black pixels) is correctly transformed to the label to be learned in the future (*e.g.*, *fan* in step-5 and *plate* in step-6) while keeping the previously learned knowledge.

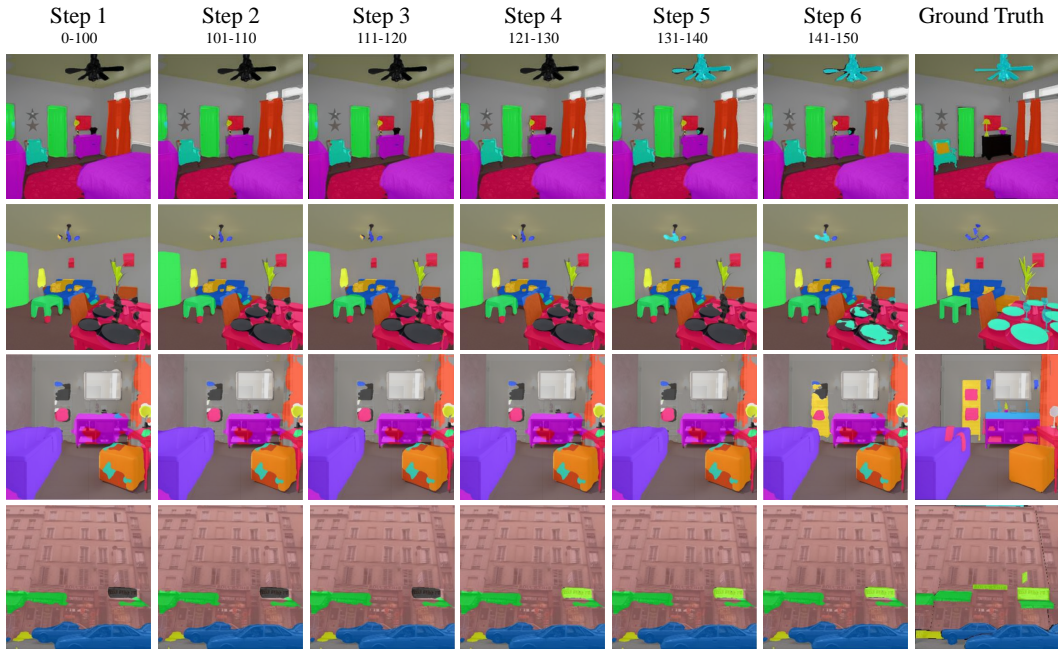


Figure 1: Qualitative results of SSUL-M on ADE20K.

References

- [1] Hongjoon Ahn, Jihwan Kwak, Subin Lim, Hyeonsu Bang, Hyojun Kim, and Taesup Moon. Ss-il: Separated softmax for incremental learning. *arXiv preprint arXiv:2003.13947*, 2020.
- [2] Holger Caesar, Jasper Uijlings, and Vittorio Ferrari. Coco-stuff: Thing and stuff classes in context. In *Proceedings of the IEEE conference on computer vision and pattern recognition*, pages 1209–1218, 2018.
- [3] Fabio Cermelli, Massimiliano Mancini, Samuel Rota Buló, Elisa Ricci, and Barbara Caputo. Modeling the background for incremental learning in semantic segmentation. In *Proceedings of the IEEE/CVF Conference on Computer Vision and Pattern Recognition*, pages 9233–9242, 2020.
- [4] Marius Cordts, Mohamed Omran, Sebastian Ramos, Timo Rehfeld, Markus Enzweiler, Rodrigo Benenson, Uwe Franke, Stefan Roth, and Bernt Schiele. The cityscapes dataset for semantic urban scene understanding. In *Proceedings of the IEEE conference on computer vision and pattern recognition*, pages 3213–3223, 2016.
- [5] Arthur Douillard, Yifu Chen, Arnaud Dapogny, and Matthieu Cord. Plop: Learning without forgetting for continual semantic segmentation. *arXiv preprint arXiv:2011.11390*, 2020.
- [6] Saihui Hou, Xinyu Pan, Chen Change Loy, Zilei Wang, and Dahua Lin. Learning a unified classifier incrementally via rebalancing. In *Proceedings of the IEEE/CVF Conference on Computer Vision and Pattern Recognition*, pages 831–839, 2019.
- [7] James Kirkpatrick, Razvan Pascanu, Neil Rabinowitz, Joel Veness, Guillaume Desjardins, Andrei A. Rusu, Kieran Milan, John Quan, Tiago Ramalho, Agnieszka Grabska-Barwinska, Demis Hassabis, Claudia Clopath, Dharshan Kumaran, and Raia Hadsell. Overcoming catastrophic forgetting in neural networks. *Proceedings of the National Academy of Sciences*, 114(13):3521–3526, 2017.
- [8] Zhizhong Li and Derek Hoiem. Learning without forgetting. *IEEE Transactions on Pattern Analysis and Machine Intelligence*, 40(12):2935–2947, 2017.
- [9] Umberto Michieli and Pietro Zanuttigh. Incremental learning techniques for semantic segmentation. In *Proceedings of the IEEE/CVF International Conference on Computer Vision Workshops*, pages 0–0, 2019.
- [10] Roozbeh Mottaghi, Xianjie Chen, Xiaobai Liu, Nam-Gyu Cho, Seong-Whan Lee, Sanja Fidler, Raquel Urtasun, and Alan Yuille. The role of context for object detection and semantic segmentation in the wild. In *Proceedings of the IEEE conference on computer vision and pattern recognition*, pages 891–898, 2014.
- [11] Nathan Silberman, Derek Hoiem, Pushmeet Kohli, and Rob Fergus. Indoor segmentation and support inference from rgb-d images. In *European conference on computer vision*, pages 746–760. Springer, 2012.